Molecular Biology of the Cell
Vol. 16, 97–105, January 2005

Coupling of Posterior Cytoskeletal Morphogenesis to the G1/S Transition in the *Trypanosoma brucei* Cell Cycle[D]

Xiaoming Tu and Ching C. Wang*

Department of Pharmaceutical Chemistry, University of California, San Francisco, CA 94143-2280

Submitted May 5, 2004; Revised October 18, 2004; Accepted October 19, 2004
Monitoring Editor: John Pringle

The expression levels of four Cdc2-related kinases (CRK1, 2, 4, and 6) in the procyclic form of *Trypanosoma brucei* were knocked down in pairs using the RNA interference (RNAi) technique. A double knockdown of CRK1 and CRK2 resulted in arrested cell growth in the G1 phase accompanied by an apparent cessation of nuclear DNA synthesis. The arrested cells became elongated at the posterior end like the G1-phase cells generated by knockdown of CycE1/CYC2 in a previous study. However, ~5% of the G1 cells in the current study also possessed multiply branched posterior ends, which have not previously been observed in *T. brucei*. DAPI and immunofluorescence staining showed a single nucleus, kinetoplast, basal body, and flagellum in the anterior portion of each G1 cell. The split and grossly extended posterior ends were heavily stained with antibodies to tyrosinated α-tubulin, suggesting an accumulation of newly synthesized microtubules. A significant population of anucleate cells (zoids), apparently derived from kinetoplast-dictated cytokinesis and cell division of the G1 cells, also had extended and branched posterior ends filled with newly synthesized microtubules. This continued posterior extension of microtubules in the G1 cells and zoids suggests that CRK1 and CRK2 exert a coordinated control on G1/S passage and the limited growth of the microtubule corset toward the posterior end. This connection may provide a new insight into the mechanism of morphological maintenance of an ancient protist during its cell cycle progression.

INTRODUCTION

Trypanosoma brucei is a parasitic protozoan and the causative agent of sleeping sickness in humans and nagana in cattle in Africa. It is also thought to be an ancient eukaryote whose lineage branched early, so that it is further removed from the mammals than are the yeasts and other fungi (Vickerman, 1994; Stevens *et al.,* 1999). *T. brucei* exhibits a specific range of cell morphologies defined by the internal cytoskeleton, which is characterized by a precisely arranged subpellicular corset of some 100 microtubules that are cross-linked to each other and to the plasma membrane (Gull, 1999). These microtubules have their plus (+) ends all pointed toward the posterior end of the cell, consistent with a postulated unified direction of cortical microtubule extension toward this end (Robinson *et al.,* 1995). Each cell also possesses a single mitochondrion that extends from the anterior all the way to the posterior end of the cell. A mitochondrial DNA complex, termed the kinetoplast, is associated across the mitochondrial membrane with the basal body, which serves as the origin of the only flagellum of the cell (Ogbadoyi *et al.,* 2003). Early in the cell cycle, the probasal body lying adjacent to the mature basal body starts to elongate and initiate growth of the new daughter flagellum. The formation of two new probasal bodies occurs only after growth of the new flagellum has been initiated. Extension of the new flagellum then continues throughout much of the cell cycle. Its close attachment to the cell body during extension, mediated by certain surface proteins (LaCount *et al.,* 2002), is believed to play an important role in cellular morphogenesis during proliferation (Sherwin and Gull, 1989). Flagellum elongation is followed by division of the kinetoplast. The two kinetoplasts thus formed and the two basal bodies then move apart within the cell. Mitosis is then initiated and followed by cytokinesis and cell separation that starts from the anterior end and terminates at the posterior end (Ploubidou *et al.,* 1999). The latter is enriched with tyrosinated α-tubulin, a marker for newly synthesized microtubules (Sherwin *et al.,* 1987), supporting the hypothesis that the microtubule corset grows toward the posterior end of the cell. The basal body also contains newly synthesized microtubules (Sherwin *et al.,* 1987), but the flagellum originated from it grows toward the anterior end of the cell. There is thus an apparent coordination between the growth of the microtubule corset and the beginning of flagellum extension in opposite directions at a certain point in the cell cycle, which appears to be in early S phase (see below).

A well-coordinated and tightly controlled cell cycle progression is essential for eukaryotic cells to maintain genomic stability and typically also to modulate and maintain normal cell morphology. The cell cycle is driven primarily by the well-controlled periodic activation and inactivation of cyclin-dependent protein kinases (CDKs) at specific checkpoints of the cell cycle (Mendenhall and Hodge, 1998; Skibbens and Hieter, 1998). The sequence of G1, S, G2, and M phases ordinarily observed among eukaryotes is also found in the cell cycle of trypanosomes, although it is regulated somewhat differently (Woodward and Gull, 1990; Li and Wang, 2003). The organism possesses four Pho80 cyclin homologues and three B-type mitotic cyclin homologues,

Article published online ahead of print. Mol. Biol. Cell 10.1091/mbc.E04–05–0368. Article and publication date are available at www.molbiolcell.org/cgi/doi/10.1091/mbc.E04–05–0368.

[D] The online version of this article contains supplemental material at MBC Online (http://www.molbiolcell.org).

* Corresponding author. E-mail address: ccwang@cgl.ucsf.edu.

but no G1 cyclin homologue (Li and Wang, 2003). In the procyclic form of *T. brucei*, which infests the midgut of infected tsetse flies, one of the Pho80 homologues, CycE1/CYC2, plays an essential role in controlling the G1/S transition. Depletion of this cyclin by RNA interference (RNAi) resulted in cells arrested in the G1 phase with the intriguing morphology of a grossly extended posterior end (Li and Wang, 2003). Approximately 10% of the cells were found in the anucleate form (the zoid), which also had an extended posterior end. Apparently, the cell cycle regulation in the procyclic form of *T. brucei* allows some of the cells arrested in the G1 phase to proceed with duplication of the kinetoplast, basal body, and flagellum, resulting in cytokinesis and cell separation (Li and Wang, 2003).

Five CDK homologues have been identified in the *T. brucei* genome and designated the Cdc2-related kinases (CRKs) 1, 2, 3, 4, and 6 (Mottram and Smith, 1995; Hammarton *et al.*, 2003a, 2003b). They have several features in common with the CDKs from yeasts and mammals, including an overall 40–50% amino acid sequence identity, a recognizable "PSTAIR" cyclin-binding box, a "DSEI" box, and the key threonine and tyrosine residues known to be the important phosphorylation sites. There are also sequences in these CRKs that distinguish them from yeast and mammalian CDKs, including N-terminal extensions in CRK2 and CRK3 and two additional domains within the catalytic site of CRK4. By RNAi experiments, CRK3 was found to play an essential role in controlling the G2/M checkpoint in both procyclic and bloodstream forms of *T. brucei* (Tu and Wang, 2004). In contrast, a knockdown of CRK1 caused only a partial enrichment of G1 cells and a corresponding decrease of the S-phase population in both forms. Although the extent of growth of the CRK1-knockdown mutant was decreased by fivefold in both forms, there was no noticeable morphological phenotype. There was also no appreciable growth inhibition or morphological phenotype in the CRK2, 4, or 6 knockdown mutant of either form. These data suggested that only CRK1 may be important in regulating the G1/S transition.

To determine if more than one CRK is involved in controlling the G1/S transition in *T. brucei*, we performed RNAi in the procyclic form to knock down expression of the CRKs in pairs. The results indicate that a combined knockdown of CRK1 and CRK2 produces a near-total growth arrest and significant accumulation of G1 cells with a unique morphological phenotype that appears to result from an uncontrolled extension of newly synthesized microtubules toward the posterior end. This suggests that these two CRKs have a dual function in coupling cell cycle progression with a controlled cytoskeleton construction.

MATERIALS AND METHODS

Cell Cultures

Procyclic-form *T. brucei* strain 29-13 cells (Wirtz *et al.*, 1999) were cultivated at 26°C in Cunningham's medium supplemented with 10% fetal bovine serum (Atlanta Biological, Lawrenceville, GA). G418 (15 μg/ml) and hygromycin B (50 μg/ml) were included in the culture medium to maintain the T7-RNA-polymerase and tetracycline-repressor gene constructs that are present in strain 29-13.

RNA Interference

Partial cDNA fragments (250–550 base pairs) of *CRK1*, *CRK2*, *CRK4*, and *CRK6* (accession numbers X64314, X74598, AJ413200, and AJ505556) were amplified by PCR using pairs of gene-specific primers (see Supplementary Table 1), and each of the six pairwise combinations was ligated together and cloned into the pZJM vector by replacing its α-tubulin fragment (Wang *et al.*, 2000). The resulting RNAi constructs were linearized with *Not*I for integration into the *T. brucei* rDNA spacer region. Transfection of strain 29-13 with the linearized DNA constructs by electroporation was performed essentially as described previously (Li *et al.*, 2002). The transfectants were selected on 2.5 μg/ml phleomycin, and individual cells were cloned by limiting dilutions on agarose plates (Carruthers and Cross, 1992). The stable transfectants thus selected were grown in culture medium containing phleomycin (Carruthers and Cross, 1992).

Transcription of the DNA insert was induced by adding 1 μg/ml tetracycline to the medium to switch on the T7 promoter. The dsRNA thus synthesized is expected to lead to specific degradation of its corresponding mRNA in *T. brucei* (Bastin *et al.*, 2000; Moreira-Leite *et al.*, 2001; Klingbeil *et al.*, 2002; Timms *et al.*, 2002). To evaluate the effects of each RNAi on cell proliferation, the cell numbers were counted at different times using a hemocytometer.

Semiquantitative RT-PCR

Total RNA was extracted from *T. brucei* cells using the TRIzol reagent (Amersham Biosciences, Piscataway, NJ) and treated with DNase I (Roche, Indianapolis, IN) to digest the remaining DNA. RT-PCR was then performed using the one-step RT-PCR kit (Invitrogen, Carlsbad, CA) and a pair of gene-specific primers that differ from the primer pair used in generating the original RNAi construct (see Supplementary Table 1).

Fluorescence-activated Cell Sorting Analysis

Cell samples for fluorescence-activated cell sorting (FACS) were prepared and analyzed as described previously (Tu and Wang, 2004). The propidium iodide (PI)-stained cell samples from FACS analysis were also examined with an Olympus phase-contrast and fluorescence microscope (Melville, NY) to tabulate the numbers of nuclei and kinetoplasts in individual cells and the numbers of cells with different morphologies in populations of ~200 cells.

BrdU Labeling and Immunofluorescence Microscopy

5-Bromo-2-deoxyuridine (BrdU) was added to the transfected, tetracycline-induced *T. brucei* cells at a concentration of 0.3 mM. Cells were harvested after 2 d of incubation, suspended gently in 100 μl phosphate-buffered saline (PBS; 137 mM NaCl, 8 mM KCl, 10 mM Na_2HPO_4, 2 mM KH_2PO_4, pH 7.4), and mixed with 200 μl of 10% ethanol/5% glycerol in PBS. They were then mixed with another 200 μl of 50% ethanol/5% glycerol before incubation on ice for 5 min. One milliliter of 70% ethanol/5% glycerol was then added, the mixture was left at 4°C overnight, and the cells were then washed twice with PBS. Immunofluorescence assays for the incorporated BrdU were then performed as described previously (Tu and Wang, 2004). Mouse anti-BrdU monoclonal antibody (mAb) and fluorescein isothiocyanate (FITC)-conjugated anti-mouse immunoglobulin G (IgG)-stained slides were mounted in Vectashield (Vector Laboratories, Burlingame, CA) in the presence of 1 μg of 4,6-diamino-2-phenylindole (DAPI) per milliliter and examined with a fluorescence microscope.

For other immunofluorescence experiments, cells were harvested, washed three times with PBS, and fixed as described above. Alternatively, they were fixed in 4% paraformaldehyde in PBS for 30 min, washed three times with PEM buffer (100 mM PIPES, 2 mM EGTA, 0.1 mM EDTA, 1 mM $MgSO_4$, pH 6.9), permeabilized with 0.1% Triton X-100 for 5 min, and washed three times with PEM buffer. Cells fixed by either protocol were blocked in blocking buffer (2% bovine serum albumin and 0.1% Triton X-100 in PBS) at room temperature for 60 min and incubated with the primary antibody at room temperature for another 60 min. The following primary antibodies were used: YL1/2 (Chemicon, Temecula, CA; rat mAb against yeast tyrosinated α-tubulin, used at 1:400 dilution); anti-CRAM (from Dr. Mary G. Lee, New York University; rabbit polyclonal antibodies against the flagellar pocket-associated cysteine-rich acidic membrane protein, used at 1:300 dilution); and ROD1 (from Dr. Keith Gull, Oxford University; mouse mAb against two paraflagellar rod [PFR] proteins; used without dilution). The FITC-conjugated goat secondary antibodies (Sigma, St. Louis, MO), including anti-rat IgG (diluted 1:400), anti-rabbit IgG (diluted 1:50), and anti-mouse IgG (diluted 1:300), were then applied as appropriate, and the cells were incubated at room temperature for another 60 min. Slides were mounted in Vectashield in the presence of 1 μg/ml DAPI and examined with a fluorescence microscope. For double staining, Cy3-conjugated goat secondary antibodies to various IgGs were used (Sigma).

RESULTS

RNAi of Pairs of CRK Genes in Procyclic-form T. brucei

We used the RNAi technique to knock down expression of the pairwise combinations of four *CRK* genes (*CRK1*, *CRK2*, *CRK4*, and *CRK6*) in the procyclic form of *T. brucei*. (*CRK3* was not included here, because its product has been shown to play a specific role in controlling the G2/M passage without any apparent involvement in the G1/S transition [Tu and Wang, 2004]). A 250- to 500-base pair DNA fragment corresponding to a unique sequence from the coding

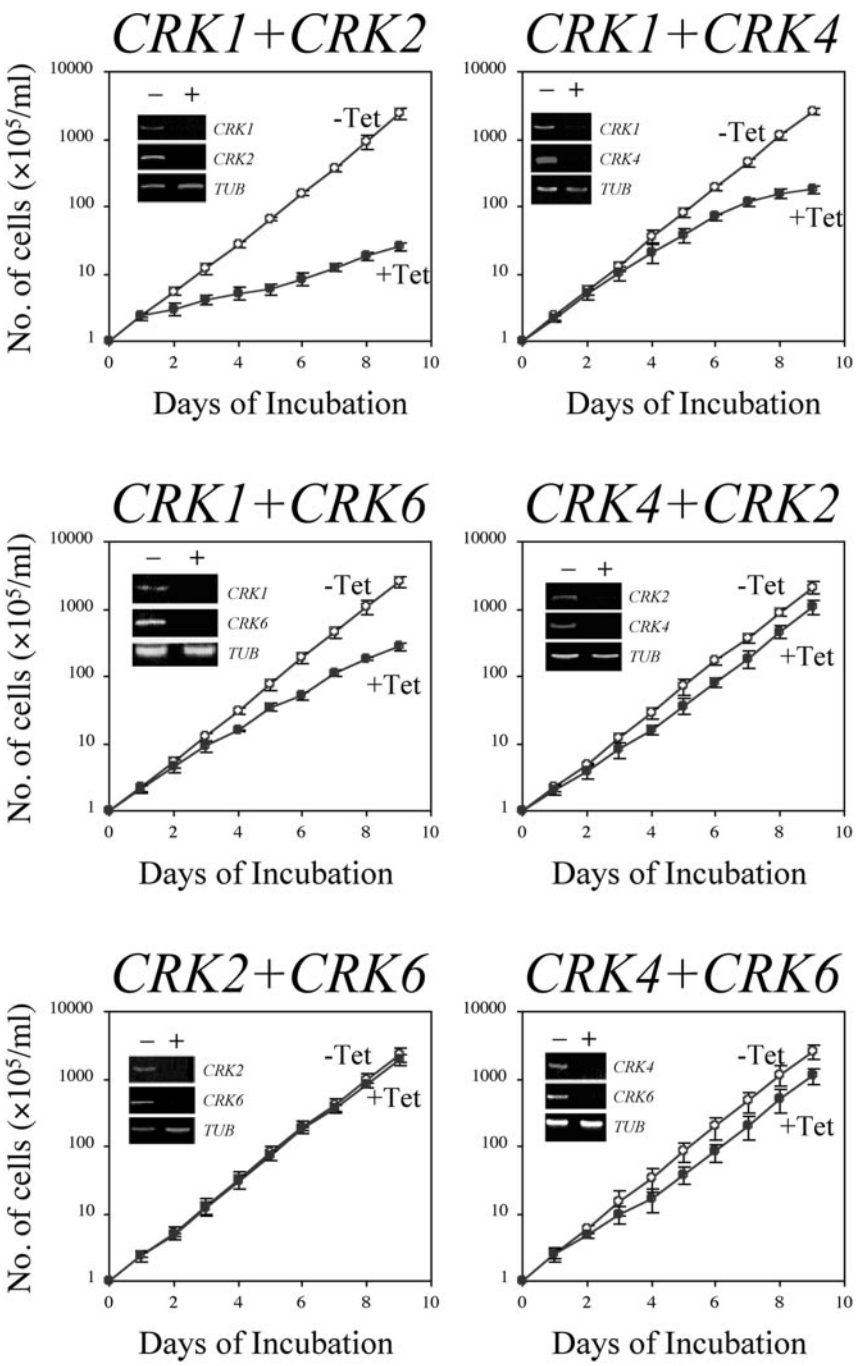

Figure 1. Effects of double CRK knockdowns on the growth of procyclic-form *T. brucei* cells. Strain 29-13 cells harboring each double-CRK-RNAi construct were incubated at 26°C in culture medium without (−Tet) or with (+Tet) 1.0 μg/ml tetracycline. The numbers of cells were monitored daily. The insets show the intracellular mRNA levels after 3 d of RNAi as monitored by semiquantitative RT-PCR. Quantitation of α-tubulin mRNA (*TUB*) was included as a control.

region of each gene, with no significant sequence identity among the rest of the genome sequences in the Trypanosome Genome Database, was amplified by PCR. Pairs of PCR fragments (CRK1+CRK2, CRK1+CRK4, CRK1+CRK6, CRK4+CRK2, CRK2+CRK6, and CRK4+CRK6) were ligated in the indicated orientation of coding strands and cloned in the RNAi vector pZJM (see *Materials and Methods*). The newly generated sequences around the junction in each pair were also compared with the Genome Database. No significant sequence identity was found, so it is highly unlikely that expression of an unidentified gene could be inadvertently knocked down by use of these constructs.

The effects of RNAi on *CRK* gene expression were examined by semiquantitative RT-PCR analysis (Figure 1, insets). In all cases, levels of the two targeted mRNAs both diminished significantly after 3 d of RNAi. The knockdowns were highly specific, as levels of the three untargeted *CRK* mRNAs remained unchanged in each case (unpublished data).

The effects of the RNAi on growth were monitored by daily counts of the numbers of transfected cells with or without tetracycline induction (Figure 1). The results indicate that a knockdown of *CRK1+CRK2* led to a significant inhibition of cell growth such that the cell number after 9 d was only 0.9% of that in the uninduced control. For the other knockdown experiments, the numbers of CRK1+CRK4-, CRK1+CRK6-, CRK4+CRK2-, CRK2+CRK6-, and CRK4+CRK6-deficient cells were reduced to 7, 11, 52, 87 and 42%, respectively, of those in the uninduced controls (Figure 1).

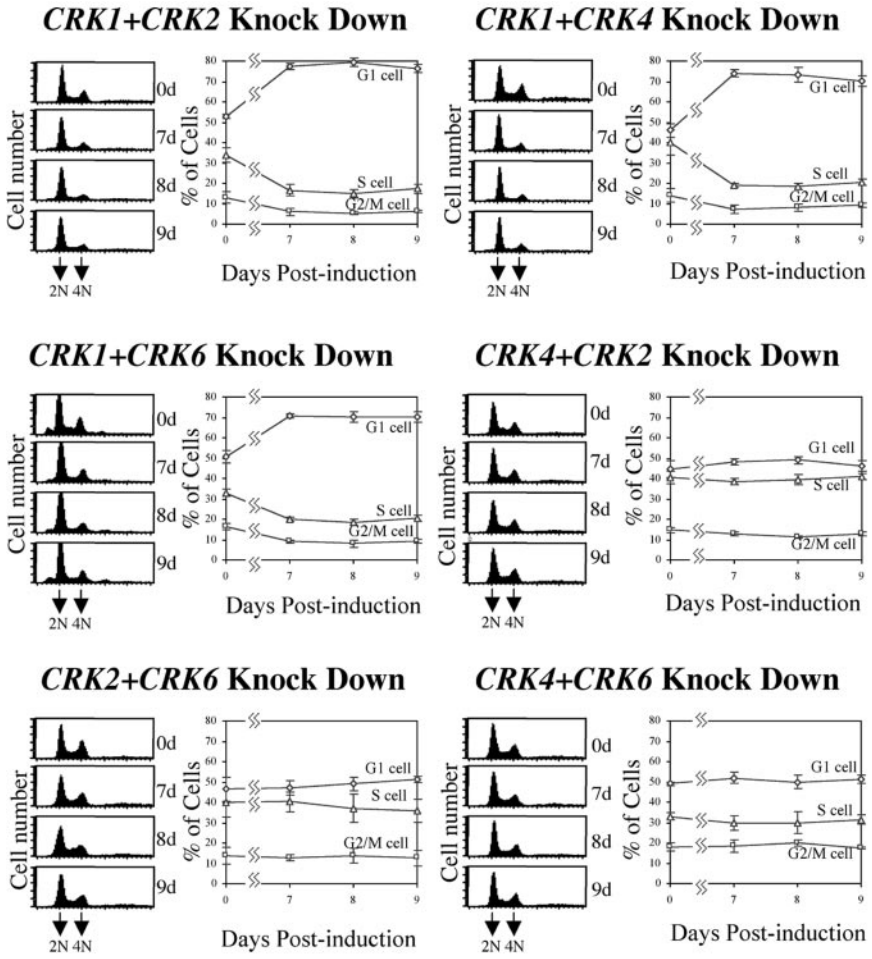

Figure 2. FACS analysis of the CRK-depleted cells. RNAi-induced cells were stained with PI and analyzed by FACS for DNA content. The plots from FACScan and the percentages of cells in G1, S, and G2/M phases (as determined by the ModFitLT software) are shown in each panel.

Effects of CRK Depletion on Cell-Cycle Progression

FACS analysis of DNA contents indicated that after 9 d of CRK1+CRK2 knockdown, G1-phase cells had increased from ~52 to 76% of the population, whereas S-phase and G2/M cells had decreased from 34 to 17% and from 14 to 7%, respectively (Figure 2). This delayed cell cycle progression reflects an additive effect of depleting the two kinases, because only relatively small changes in cell cycle distributions were observed previously upon knocking down either *CRK1* or *CRK2* alone (Tu and Wang, 2004). The double depletion of CRK1+CRK4 or CRK1+CRK6 produced similar changes in cell cycle distribution (Figure 2), whereas double depletion of CRK4+CRK2, CRK2+CRK6, or CRK4+CRK6 produced only very marginal changes. Taken together, these data suggest that CRK1 is the central kinase regulating the G1/S transition and that CRK2, CRK4, and CRK6 can all play an auxiliary role in potentiating its action. The more severe growth inhibition observed with the CRK1+CRK2 double knockdown might reflect a CRK2 function in promoting cell growth unrelated to regulation of the G1/S transition. However, the absence of any detectable growth inhibition either with CRK2 depletion alone (Tu and Wang, 2004) or with CRK4+CRK2 or CRK2+CRK6 double knockdown (Figure 1) argues against this interpretation. Thus, the stronger growth inhibition in CRK1+CRK2-deficient cells may simply reflect a stronger G1/S delay, an interpretation that is supported by the data on BrdU incorporation and morphological examination as described below.

Unusual Morphologies of the CRK1+CRK2-deficient Cells

The PI-stained CRK-depleted cells were examined by fluorescence microscopy to tabulate the cells with one nucleus+one kinetoplast (1N1K), one nucleus+two kinetoplasts (1N2K), two nuclei+two kinetoplasts (2N2K), or no nucleus+one kinetoplast (0N1K, the zoids). The CRK4+CRK2-, CRK2+CRK6-, and CRK4+CRK6-depleted cells showed little change in the distribution of cell morphologies during 5 d of RNAi (unpublished data). In contrast, the CRK1+CRK2-, CRK1+CRK4-, and CRK1+CRK6-depleted cells showed increases of 1N1K cells and corresponding decreases of 1N2K and 2N2K cells (Figure 3A and unpublished data), consistent with the postulated delay in the G1/S transition in these cells. No 2N1K cells were detected, indicating that the kinetoplast cycle is undisturbed in these cells.

Although the CRK1+CRK4- and CRK1+CRK6-deficient cells displayed apparently normal morphologies without a detectable zoid population (unpublished data), the CRK1+CRK2-depleted cell population contained ~10% zoids (Figure 3, A and D) and many other cells with abnormal morphologies. In particular, although approximately half of the 1N1K cells retained normal morphology (Figure 3B), 41% possessed a grossly elongated posterior end after 5 d of RNAi (Figure 3, B and D), like the 1N1K cells in the CycE1/CYC2-depleted procyclic-form cells (Li and Wang, 2003). An additional 6% of the 1N1K population had not only an elongated posterior end but also two branches of it, whereas ~1% had multiple branches of the elongated pos-

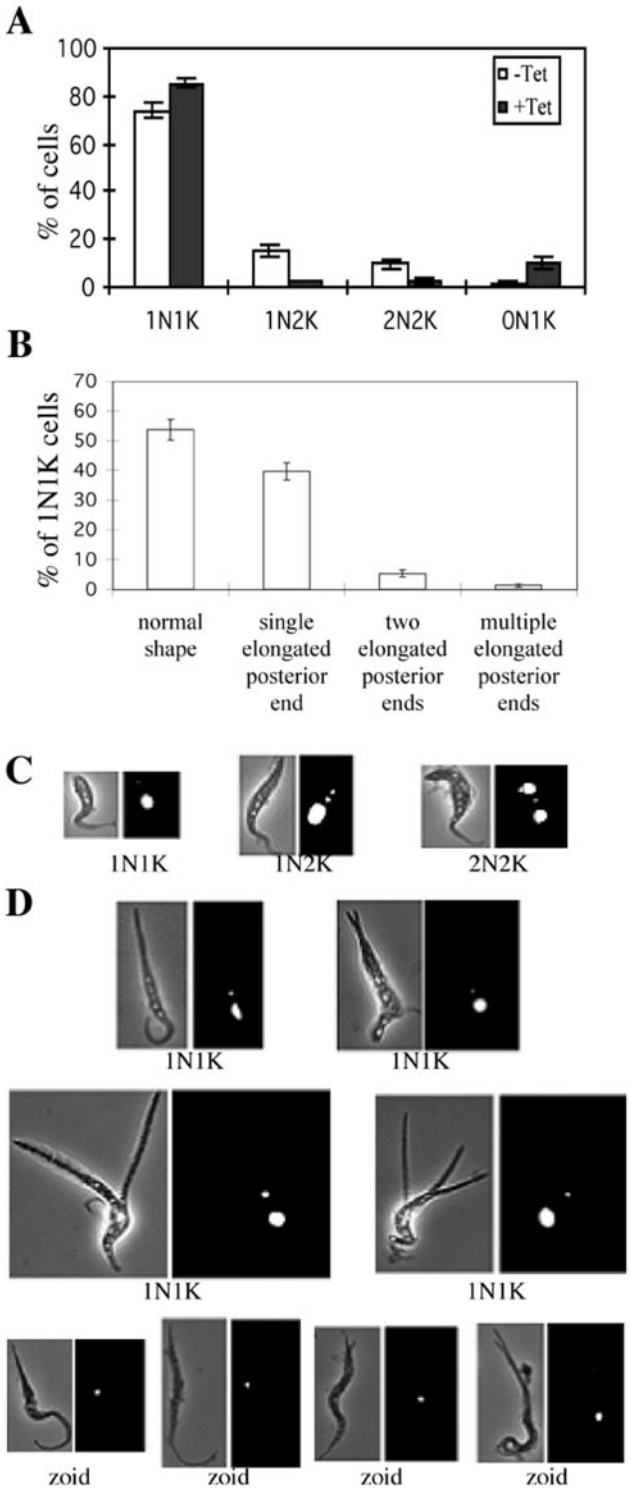

Figure 3. Morphological phenotypes of CRK1+CRK2-deficient cells. Strain 29-13 cells after 5 d of RNAi for CRK1 and CRK2 were stained with PI and examined by fluorescence microscopy. (A and B) Quantification of cells (A) with different numbers of nuclei (N) and kinetoplasts (K) and (B) with different morphologies in the 1N1K population. Data are presented as the mean percentages ±SE for the total populations counted (>200 cells in each of three independent experiments). (C and D) Examples of different cell types identified in the wild-type (C) and CRK1+CRK2-depleted (D) populations. All cells are oriented with their posterior ends pointing upward.

terior end (Figure 3, B and D). The lengths of the paired branches were roughly equal but ranged from very short to very long (Figure 3D). As RNAi induction was prolonged from 3 to 5 and 7 d, there was a progressive increase in the number of cells with longer posterior branches (unpublished data), suggesting a chronology from an initially split posterior end to a lengthening of the branches. The multiple branches were often quite long and did not always originate from the same site at the posterior end (Figure 3D). A new branch could also grow from an existing branch, giving a tree-like appearance (see Figure 6B).

The emergence of up to 10% zoids in the CRK1+CRK2-deficient population suggests that some of the G1-arrested cells can still complete cell division, presumably driven by the kinetoplast cycle, resulting in anucleate daughter cells, as observed previously in CycE1/CYC2-depleted cells (Li and Wang, 2003). All zoids in the present experiments also had grossly extended posterior ends (Figure 3D), similar to the previously observed slender zoids (Li and Wang, 2003). However, 5% of the elongated zoids seen here also had a split posterior end (Figure 3D), which was not observed previously. These branches were generally very short and restricted to only two per cell, suggesting that a continuing extension of the posterior branches may not be possible in the absence of a nucleus.

BrdU Incorporation in CRK1+CRK2-deficient Cells

To determine if all the 1N1K cells in the CRK-knockdown populations are genuinely arrested in the G1 phase and prevented from nuclear DNA synthesis, BrdU was added to the cells after 3 d of RNAi, and the cells were examined 2 d later for BrdU incorporation into DNA. The 1N1K cells of normal morphology (Figure 4B, top cell) appeared to incorporate BrdU into the nucleus essentially as did the uninduced cells (Figure 4A). Thus, these cells, which constitute ~50% of the 1N1K population after 5 d of RNAi (see Figure 3B), are not really arrested in G1 phase and are apparently capable of entering S phase. They may be growing slowly and may be responsible for the residual cell proliferation observed in Figure 1. In contrast, in the 1N1K cells with an elongated or branched posterior end, there was no detectable incorporation of BrdU into nuclear DNA (Figure 4B, lower three cells). Thus, these cells were probably truly arrested in G1 phase. It appears that when BrdU was added after 3 d of RNAi, the population was heterogeneous: some cells were only partially depleted of CRK1+CRK2 and thus were still progressing slowly through the cell cycle, whereas the others were truly arrested in G1.

In the CRK1+CRK4- and CRK1+CRK6-knockdown populations, all 1N1K cells had normal morphology, and the incorporation of BrdU into the nuclei was indistinguishable from that in uninduced control cells (Figure 4, C and D). Thus, the apparent enrichment of G1 cells in these cases (Figure 2) appears to be due largely or entirely to a slower passage of cells across the G1/S boundary rather than to any subpopulation that is genuinely arrested in G1.

Further Characterization of the CRK1+CRK2-depleted Cells

Because the morphology of a trypanosome cell is defined primarily by its microtubule cytoskeleton (Gull, 1999), the cells with extended posterior ends were examined by immunofluorescence microscopy using YL1/2, an antibody specific for tyrosinated α-tubulin (Kilmartin *et al.*, 1982; Wehland *et al.*, 1983). This antibody stains both the basal bodies and the newly assembled microtubules at the posterior end of trypanosome cells (Sherwin *et al.*, 1987). As

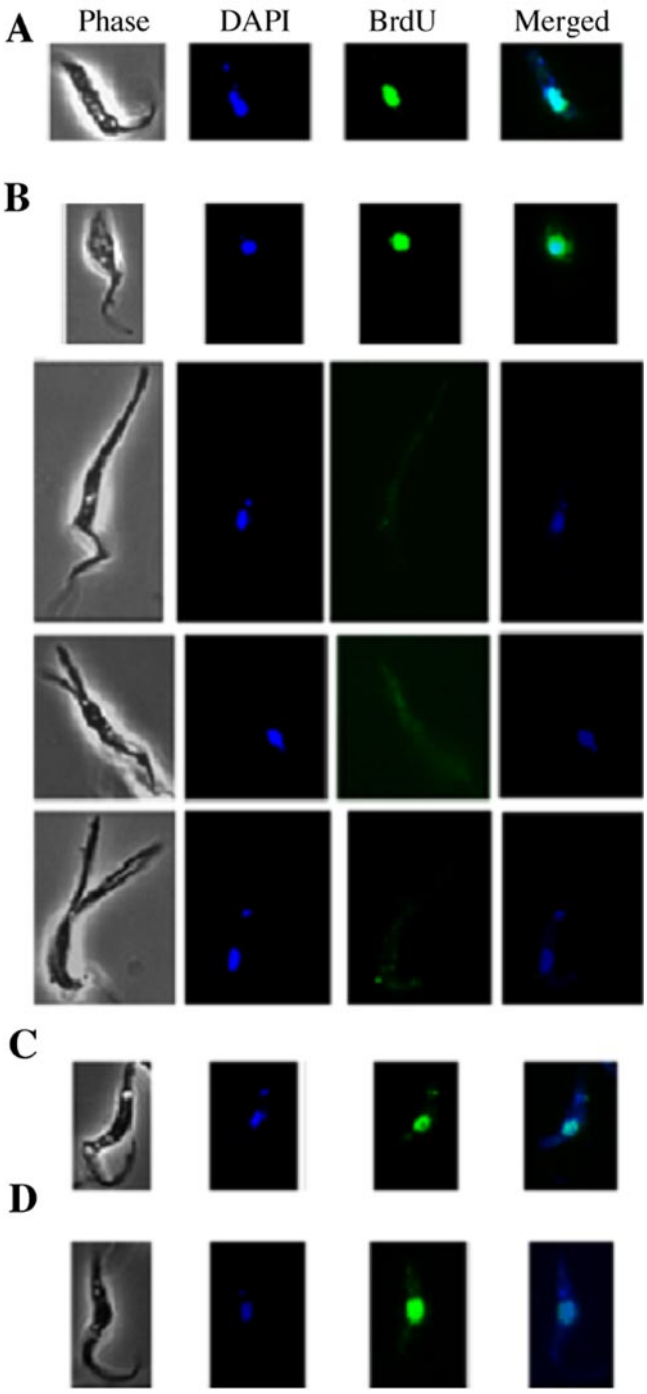

Figure 4. BrdU incorporation in control and RNAi-treated cells. BrdU was added to strain 29-13 cells 3 d after RNAi induction, and the cells were harvested 2 d later. Images from the anti-BrdU immunofluorescence assays were recorded and superimposed on the DAPI staining patterns. All cells are oriented with their posterior ends pointing upward. (A) A control cell. (B) CRK1+CRK2-deficient cells. (C) A CRK1+CRK4-deficient cell. (D) A CRK1+CRK6-deficient cell. Note that BrdU only failed to incorporate into the nuclei of cells with elongated posterior ends.

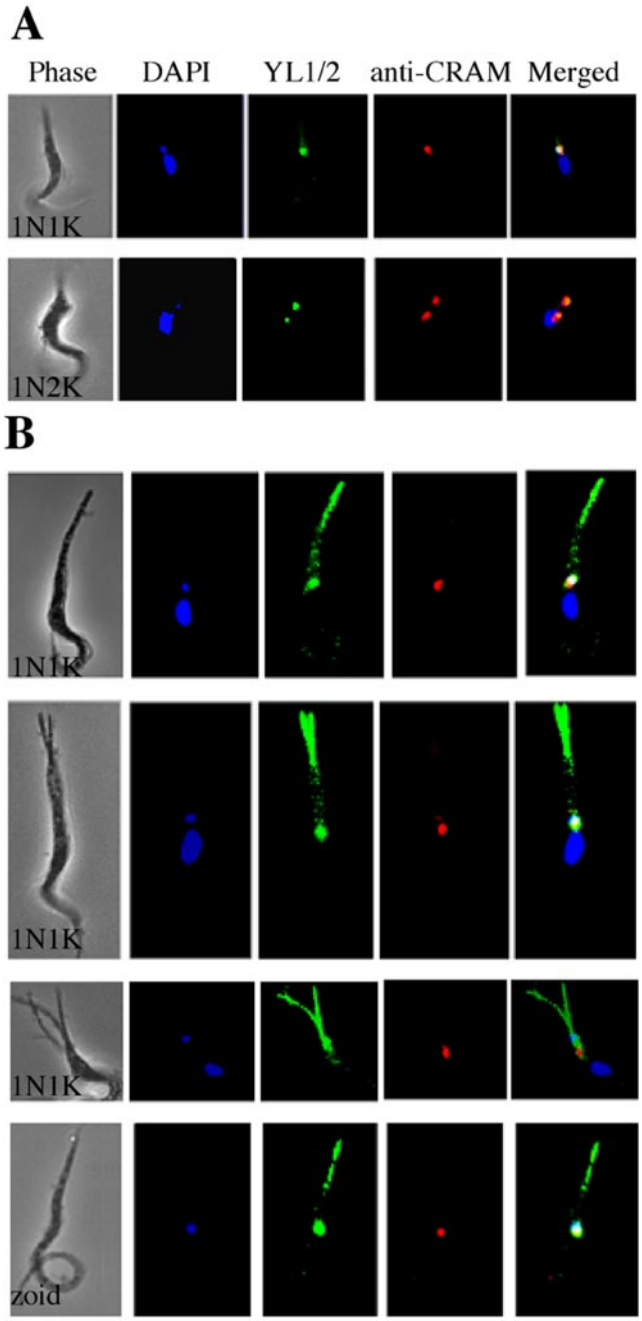

Figure 5. Localization of newly assembled microtubules in CRK1+CRK2-depleted cells of abnormal morphology. Strain 29-13 cells after 5 d of CRK1+CRK2 RNAi were stained with DAPI, YL1/2 for tyrosinated α-tubulin, and anti-CRAM for the flagellar pocket and examined by fluorescence microscopy. All cells are oriented with their posterior end pointing upward. (A) 1N1K and 1N2K control cells without RNAi induction. (B) CRK1+CRK2-deficient 1N1K cells and a zoid with elongated and/or multiple posterior ends.

expected (Gull, 1999; Liu *et al.*, 2000), in control 1N1K and 1N2K cells, the staining revealed one and two basal bodies, respectively, each of which was closely associated with a DAPI-stained kinetoplast and a flagellar pocket that stained with the anti-CRAM antibody (Figure 5A). In the CRK1+CRK2-depleted 1N1K cells with elongated posterior ends, overlapping staining of a single basal body, a single kinetoplast, and a single flagellar pocket was seen as in the control cells (Figure 5B, upper three cells). In addition, how-

ever, the elongated posterior ends were heavily stained with the YL1/2 antibody in a pattern that was largely absent from the normal posterior ends of control cells (Figure 5A). This seemingly massive accumulation of newly synthesized microtubules in the single and multiple extended posterior ends is presumably a consequence of the cells' being trapped in G1 by depletion of both CRK1 and CRK2. The zoids also showed colocalization of a single kinetoplast, basal body, and flagellar pocket, and an extended posterior end filled with newly synthesized microtubules (Figure 5B, bottom cell).

The antiparaflagellar-rod-protein antibody ROD1, which specifically stains the flagellum of *T. brucei* (Woods *et al.*, 1989), was also used in immunofluorescence. As expected, a single flagellum was found to be associated with the anterior portion of control 1N1K and 1N2K cells (Figure 6A). Results with the elongated CRK1+CRK2-depleted 1N1K cells and zoids were similar (Figure 6B). There was no indication of duplicated, altered, or dislocated flagella in these cells, suggesting that the massive assembly of new microtubules at the posterior ends is restricted in both its location and its consequences. This conclusion agrees with previous data indicating that cytoskeleton elongation and flagellum formation are two separate processes in trypanosomes (Kohl *et al.*, 2003). The presence of a single flagellum in the zoids suggests that duplication of the flagellum did occur among some of the cells trapped in G1, resulting in cell division and the generation of anucleate cells.

DISCUSSION

In this study, we have shown that knocking down the expression of CRK1 plus another CRK causes an accumulation of G1-phase cells in the procyclic form of *T. brucei*. This accumulation is substantially more extreme than that observed in cells with just one CRK knocked down (Tu and Wang, 2004), suggesting that the CRKs overlap in function. For the CRK1+CRK4 and CRK1+CRK6 double knockdowns, this accumulation in G1 appears to be due largely to a slower passage through the G1/S transition: the cells can still synthesize nuclear DNA and have normal morphology. For the CRK1+CRK2-knockdown cells, about half of the 1N1K cells also appear to continue cycling: they are still capable of incorporating BrdU into nuclear DNA after 3 d of RNAi, and they have a normal morphology. In contrast, the rest of the 1N1K cells have elongated or multiple elongated posterior ends and are no longer capable of DNA synthesis, suggesting that they are trapped in the G1 phase. An intriguing question is why the G1-arrested cells always display such abnormal posterior ends.

Procyclic-form *T. brucei* cells with extended posterior ends were first observed among cells overexpressing TbZFP2, a member of the CCCH zinc-finger protein family (Hendriks *et al.*, 2001). The phenotype, termed the "nozzle" by the authors, involved a polar extension of microtubules at the posterior ends of cells that were apparently arrested in an early phase of the cell cycle. In a previous study in which CycE1/CYC2 expression was knocked down, we also observed an arrest in G1 and elongated posterior ends (Li and Wang, 2003), which were also subsequently found to contain newly synthesized microtubules (Hammarton *et al.*, 2004). Thus, in three distinct cases in which procyclic-form *T. brucei* cells have been arrested early in the cell cycle, similar posterior extensions have been observed. The ultrastructure of the "nozzle" was examined by transmission electron microscopy and appeared to involve a bundle of parallel microtubules (Hendriks *et al.*, 2001). From their similar immunostaining patterns with YL1/2 antibody, the extended posterior ends in the CycE1/CYC2- and CRK1+CRK2-knockdown mutants are likely to have a similar ultrastruc-

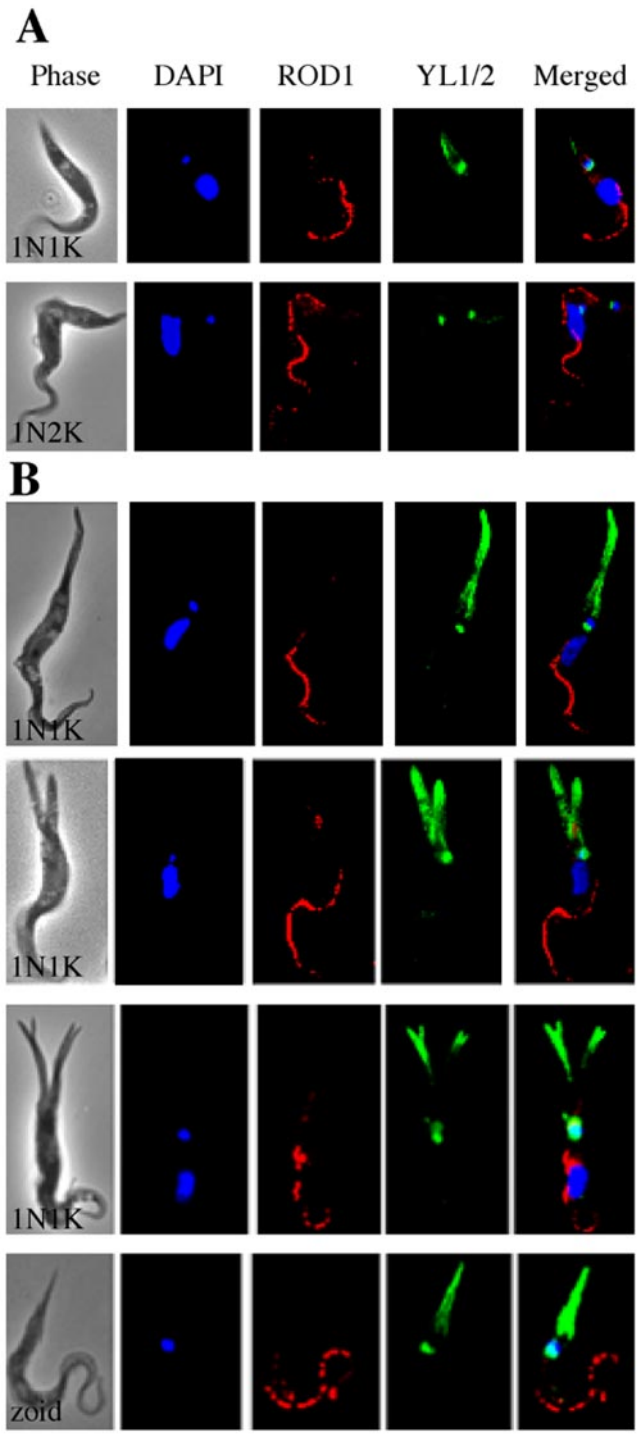

Figure 6. Flagellar localization and structure in CRK1+CRK2-depleted cells. Strain 29-13 cells after 5 d of CRK1+CRK2 RNAi were stained with DAPI, YL1/2 for tyrosinated α-tubulin, and ROD1 for the flagellum and examined by fluorescence microscopy. All cells are oriented with their posterior ends pointing upward. (A) 1N1K and 1N2K control cells without RNAi induction. (B) CRK1+CRK2-deficient 1N1K cells and a zoid with elongated and/or multiple posterior ends.

ture. The branched posterior ends in the CRK1+CRK2-knockdown mutant may result from a further uneven growth among the microtubules. TbZFP2 is known to contain an E3 ubiquitin ligase-like domain (Hendriks *et al.*, 2001). If this protein is involved in ubiquitinating CycE1/CYC2, its overexpression could lead to excessive proteasomal degradation of this cyclin, resulting in a G1 arrest and the resulting morphological changes.

There are more than 100 microtubules underlying the membrane and forming the subpellicular corset in *T. brucei* cells (Hemphill *et al.*, 1991). These microtubules are arranged in a helical pattern along the long axis of the cell and are evenly spaced and cross-linked to each other and to the membrane (Kohl and Gull, 1998). They all appear to have the same polarity, with their plus (+) ends located at the posterior end of the cell (Robinson *et al.*, 1995). This explains why the YL1/2 antibody, which recognizes tyrosinated α-tubulin, stains only the posterior end and the basal body in *T. brucei* cells, because the newly synthesized microtubules are presumably located at these sites.

CRK1 and CRK2 of *T. brucei* are 34- and 39-kDa proteins that have ~50% sequence identity with *Schizosaccharomyces pombe* Cdc2p and human CDK2 (Morgan, 1997; Tu and Wang, 2004), which are both involved in regulating the G1/S transition. CRK1 has 84% sequence identity with *Trypanosoma cruzi* TzCRK1, which is known to coimmunoprecipitate with mammalian cyclins E, D3, and A and interact with the three *T. cruzi* Pho80-like cyclins TzCYC4, 5, and 6 (Gómez *et al.*, 1998, 2001) and was postulated to have a role in regulating the G1/S transition.

If CRK1 and CRK2 function similarly in *T. brucei*, how might their depletion result in the abnormal morphologies observed? CDKs are known to phosphorylate microtubule-associated proteins to convert the interphase microtubules to the shorter and more dynamic mitotic microtubules in animal cells (Lamb *et al.*, 1990; Verde *et al.*, 1990; Vandre *et al.*, 1991; Ookata *et al.*, 1995), and a Cdc2 homologue was recently found to be associated with the cortical microtubules in protoplasts of carrot, tobacco, and *Arabidopsis* cells (Hemsley *et al.*, 2001). Thus, CDKs may associate with microtubules and, in this way, exert regulatory effects on cytoskeletal biogenesis.

Initiation of S phase in *T. brucei* is signaled by an elongation of the probasal body into a mature new basal body and the growth from it of a daughter flagellum toward the anterior end of the cell (Kohl and Gull, 1998). These events are presumably triggered and controlled by the G1/S regulatory proteins, which, from the data presented above, appear to include both CRK1 and CRK2 in *T. brucei*. Thus, in the cells arrested in G1 by depletion of CRK1 and CRK2, there is no new basal body formed and no synthesis of the new flagellum, except perhaps in the mothers of zoids. Meanwhile, the continued extension of the cortical microtubules in the posterior direction is not turned off, leading to an uncontrolled extension of the posterior end. The branching of the posterior ends, presumably reflecting an uneven extension among the parallel microtubules, could be a built-in mechanism for morphological cytoskeleton modulation (Robinson *et al.*, 1995). It is not yet clear, however, why G1 cells arrested by CycE1/CYC2 depletion do not appear to have the branched posterior growth (Li and Wang, 2003). One possible explanation is that a more extensive loss of control over the posterior extension could result from the CRK1+CRK2 knockdown, reflecting a potential role of CRK1/CRK2 in controlling microtubule assembly.

The presence of extended posterior ends in the zoids generated from both CycE1/CYC2- (Li and Wang, 2003) and CRK1+CRK2-knockdown cells indicates that cortical microtubule extension can continue also in the anucleate cells. Furthermore, because the zoid possesses a kinetoplast, a basal body, and a flagellum, duplication of these organelles must take place in the G1-arrested 1N1K cells in order for subsequent cell division to produce a zoid. A similar observation was made on procyclic-form *T. brucei* cells arrested in G1 by aphidicolin (Ploubidou *et al.*, 1999), which also produced zoids. Among the aphidicolin-arrested 1N1K cells, 90% contained one basal body, whereas 10% possessed two, supporting the hypothesis that replication of the basal body can be independent of the nuclear S-phase. Thus, a procyclic-form *T. brucei* cell arrested in G1 can still proceed with cortical microtubule extension and with synthesis of kinetoplast, basal body, and the new flagellum, leading eventually to cytokinesis and cell division. Thus, the regulation of cell cycle progression in the trypanosome appears to be quite loose in comparison with the tightly coupled cell cycle–dependent events of centrosome duplication, mitosis, and cytokinesis as seen in yeast and metazoa.

In conclusion, we have identified in procyclic-form *T. brucei* cells a combined CRK1+CRK2 regulation of the G1/S transition as well as a cell cycle-dependent inhibition of cortical microtubule growth toward the posterior end. The accumulated evidence suggests a well-coordinated regulation between cell cycle progression and cytoskeleton modulation in this ancient protist.

ACKNOWLEDGMENTS

We thank Professor W. Zacheus Cande of the University of California, Berkeley, for his valuable and stimulating discussions with us during the progress of this work and for his most helpful comments and suggestions on the manuscript. We are also grateful to Dr. Kent Hill of UCLA for his inspiring comments on the work. Gratitude goes also to the generous gifts of anti-CRAM from Dr. Mary G. Lee of New York University and ROD1 from Dr. Keith Gull of Oxford University. This study was supported by National Institutes of Health grant AI-21786.

REFERENCES

Bastin, P., Ellis, K., Kohl, L., and Gull, K. (2000). Flagellum ontogeny in trypanosomes studied via an inherited and regulated RNA interference system. J. Cell Sci. *113*, 3321–3328.

Carruthers, V. B., and Cross, G. A. (1992). High-efficiency clonal growth of bloodstream- and insect-form *Trypanosoma brucei* on agarose plates. Proc. Natl. Acad. Sci. USA *89*, 8818–8821.

Gómez, E. B., Kornblihtt, A. R., and Téllez-Iñón, M. T. (1998). Cloning of a cdc2-related protein kinase from *Trypanosoma cruzi* that interacts with mammalian cyclins. Mol. Biochem. Parasitol. *91*, 337–351.

Gómez, E. B., Santori, M. I., Laria, S., Engel, J. C., Swindle, J., Eisen, H., Szankasi, P., and Téllez-Iñón, M. T. (2001). Characterization of the *Trypanosoma cruzi* Cdc2p-related protein kinase 1 and identification of three novel associating cyclins. Mol. Biochem. Parasitol. *113*, 97–108.

Gull, K. (1999). The cytoskeleton of trypanosomatid parasites. Annu. Rev. Microbiol. *53*, 629–655.

Hammarton, T. C., Clark, J., Douglas, F., Boshart, M., and Mottram, J.C. (2003a). Stage-specific differences in cell cycle control in *Trypanosoma brucei* revealed by RNA interference of a mitotic cyclin. J. Biol. Chem. *278*, 22877–22886.

Hammarton, T. C., Mottram, J. C., and Doerig, C. D. (2003b). The cell cycle of parasitic protozoa: potential for chemotherapeutic exploitation. Prog. Cell Cycle Res. *5*, 91–101.

Hammarton, T. C., Engstler, M., and Mottram, J. C. (2004). The *Trypanosoma brucei* cyclin, CYC2, is required for cell cycle progression through G1 phase and for maintenance of procyclic form cell morphology. J. Biol. Chem. *279*, 24757–24764.

Hemphill, A., Lawson, D., and Seebeck, T. (1991). The cytoskeletal architecture of *Trypanosoma brucei*. J. Parasitol. *77*, 603–612.

Hemsley, R., McCutcheon, S., Doonan, J., and Lloyd, C. (2001). P34^{cdc2} kinase is associated with cortical microtubules from higher plant protoplasts. FEBS Lett. *508*, 157–161.

Hendriks, E. F., Robinson, D. R., Hinkins, M., and Matthews, K. R. (2001). A novel CCCH protein which modulates differentiation of *Trypanosoma brucei* to its procyclic form. EMBO J. *20*, 6700–6711.

Kilmartin, J. V., Wright, B., and Milstein, C. (1982). Rat monoclonal antitubulin antibodies derived by using a new nonsecreting rat cell line. J. Cell Biol. *93*, 576–582.

Klingbeil, M. M., Motyka, S. A., and Englund, P. T. (2002). Multiple mitochondrial DNA polymerases in *Trypanosoma brucei.* Mol. Cell *10*, 175–186.

Kohl, L., and Gull, K. (1998). Molecular architecture of the trypanosome cytoskeleton. Mol. Biochem. Parasitol. *93*, 1–9.

Kohl, L., Robinson, D., and Bastin, P. (2003). Novel roles for the flagellum in cell morphogenesis and cytokinesis of trypanosomes. EMBO J. *22*, 5336–5346.

LaCount, D. J., Barrett, B., and Donelson, J. E. (2002). *Trypanosoma brucei* FLA1 is required for flagellum attachment and cytokinesis. J. Biol. Chem. *277*, 17580–17588.

Lamb, N. J., Fernandez, A., Watrin, A., Labbe, J. C., and Cavadore, J. C. (1990). Microinjection of p34^{cdc2} kinase induces marked changes in cell shape, cytoskeletal organization, and chromatin structure in mammalian fibroblasts. Cell *60*, 151–165.

Li, Z., Zou, C-B., Yao, Y., Hoyt, M. A., McDonough, S., Mackey, Z. B., Coffino, P., and Wang, C. C. (2002). An easily dissociated 26S proteasome catalyzes an essential ubiquitin-mediated protein degradation pathway in *Trypanosoma brucei.* J. Biol. Chem. *277*, 15486–15498.

Li, Z., and Wang, C. C. (2003). A PHO80-like cyclin and a B-type cyclin control the cell cycle of the procyclic form of *Trypanosoma brucei.* J. Biol. Chem. *278*, 20652–20658.

Liu, J., Qiao, X., Du, D., and Lee, M. G. (2000). Receptor-mediated endocytosis in the procyclic form of *Trypanosoma brucei.* J. Biol. Chem. *275*, 12032–12040.

Mendenhall, M. D., and Hodge, A. E. (1998). Regulation of Cdc28 cyclin-dependent protein kinase activity during the cell cycle of the yeast *Saccharomyces cerevisiae.* Microbiol. Mol. Biol. Rev. *62*, 1191–1243.

Moreira-Leite, F. F., Sherwin, T., Kohl, L., and Gull, K. (2001). A trypanosome structure involved in transmitting cytoplasmic information during cell division. Science *294*, 610–612.

Morgan, D. O. (1997). Cyclin-dependent kinases: engines, clocks, and microprocessors. Annu. Rev. Cell Dev. Biol. *13*, 261–291.

Mottram, J. C., and Smith, G. (1995). A family of trypanosome cdc2-related protein kinases. Gene *162*, 147–152.

Mottram, J. C., McCready, B. P., Brown, K. P., and Grant, K. M. (1996). Gene disruptions indicate an essential function for the LmmCRK1 cdc2-related kinase of *Leishmania mexicana.* Mol. Microbiol. *22*, 573–582.

Ogbadoyi, E. O., Robinson, D. R., and Gull, K. (2003). A high-order transmembrane structural linkage is responsible for mitochondrial genome positioning and segregation by flagellar basal bodies in trypanosomes. Mol. Biol. Cell *14*, 1769–1779.

Ookata, K., Hisanaga, S., Bulinski, J. C., Murofushi, H., Aizawa, H., Itoh, T. J., Hotani, H., Okumura, E., Tachibana, K., and Kishimoto, T. (1995). Cyclin B interaction with microtubule-associated protein 4 (MAP4) targets p34^{cdc2} kinase to microtubules and is a potential regulator of M-phase microtubule dynamics. J. Cell Biol. *128*, 849–862.

Ploubidou, A., Robinson, D. R., Docherty, R. C., Ogbadoyi, E. O., and Gull, K. (1999). Evidence for novel cell cycle checkpoint in trypanosomes: kinetoplast segregation and cytokinesis in the absence of mitosis. J. Cell Sci. *112*, 4641–4650.

Robinson, D. R., and Gull, K. (1991). Basal body movements as a mechanism for mitochondrial genome segregation in the trypanosome cell cycle. Nature *352*, 731–733.

Robinson, D. R., Sherwin, T., Ploubidou, A., Byard, E. H., and Gull, K. (1995). Microtubule polarity and dynamics in the control of organelle positioning, segregation, and cytokinesis in the trypanosome cell cycle. J. Cell Biol. *128*, 1163–1172.

Sherwin, T., Schneider, A., Sasse, R., Seebeck, T., and Gull, K. (1987). Distinct localization and cell cycle dependence of COOH terminally tyrosinolated α-tubulin in the microtubules of *Trypanosoma brucei brucei.* J. Cell Biol. *104*, 439–446.

Sherwin, T., and Gull, K. (1989). The cell division cycle of *Trypanosoma brucei brucei*: timing of event marker and cytoskeletal modulations. Phil. Trans. Royal Soc. Lond. *323*, 573–588.

Skibbens, R. V., and Hieter, P. (1998). Kinetochores and the checkpoint mechanism that monitors for defects in the chromosome segregation machinery. Annu. Rev. Genet. *32*, 307–337.

Stevens, J. R., Noyes, H. A., Dover, G. A., and Gibson, W. C. (1999). The ancient and divergent origins of the human pathogenic trypanosomes, *Trypanosoma brucei* and *T. cruzi.* Parasitology *118*, 107–116.

Timms, M. W., van Deursen, F. J., Hendriks, E. F., and Matthews, K. R. (2002). Mitochondrial development during life cycle differentiation of African trypanosomes: evidence for a kinetoplast-dependent differentiation control point. Mol. Biol. Cell *13*, 3747–3759.

Tu, X. M., and Wang, C. C. (2004). The involvement of two cdc2-related kinases (CRKs) in *Trypanosoma brucei* cell cycle regulation and the distinctive stage-specific phenotypes caused by CRK3 depletion. J. Biol. Chem. *279*, 20519–20528.

Vandre, D. D., Centonze, V. E., Peloquin, J., Tombes, R. M., and Borisy, G. G. (1991). Proteins of the mammalian mitotic spindle: phosphorylation/dephosphorylation of MAP-4 during mitosis. J. Cell Sci. *98*, 577–588.

Verde, F., Labbé, J.-C., Dorée, M., and Karsenti, E. (1990). Regulation of microtubule dynamics by cdc2 protein kinase in cell-free extracts of *Xenopus* eggs. Nature *343*, 233–238.

Vickerman, K. (1994). The evolutionary expansion of the trypanosomatid flagellates. Int. J. Parasitol. *24*, 1317–1331.

Wang, Z., Morris, J. C., Drew, M. E., and Englund, P. T. (2000). Inhibition of *Trypanosoma brucei* gene expression by RNA interference using an integratable vector with opposing T7 promoters. J. Biol. Chem. *275*, 40174–40179.

Wehland, J., Willingham, M. C., and Sandoval, I. V. (1983). A rat mAb reacting specifically with the tyrosylated form of α-tubulin. I. Biochemical characterization, effects on microtubule polymerization in vitro, and microtubule polymerization and organization in vivo. J. Cell Biol. *97*, 1467–1475.

Wirtz, E., Leal, S., Ochatt, C., and Cross, G. A. (1999). A tightly regulated inducible expression system for conditional gene knock-outs and dominant-negative genetics in *Trypanosoma brucei.* Mol. Biochem. Parasitol. *99*, 89–101.

Woods, A., Sherwin, T., Sasse, R., MacRae, T. H., Baines, A. J., and Gull, K. (1989). Definition of individual components within the cytoskeleton of *Trypanosoma brucei* by a library of monoclonal antibodies. J. Cell Sci. *93*, 491–500.

Woodward, R., and Gull, K. (1990). Timing of nuclear and kinetoplast DNA replication and early morphological events in the cell cycle of *Trypanosoma brucei.* J. Cell Sci. *95*, 49–57.